HHS Public Access

Author manuscript

ACS Nano. Author manuscript; available in PMC 2017 August 31.

Published in final edited form as:

ACS Nano. 2017 January 24; 11(1): 153–162. doi:10.1021/acsnano.6b06200.

Cross-Linked Fluorescent Supramolecular Nanoparticles as Finite Tattoo Pigments with Controllable Intradermal Retention Times

Jin-sil Choi[†], **Yazhen Zhu**[†,‡], **Hongsheng Li**[§], **Parham Peyda**[†], **Thuy Tien Nguyen**[†], **Mo Yuan Shen**[⊥], **Yang Michael Yang**[‖], **Jingyi Zhu**[§], **Mei Liu**[§], **Mandy M. Lee**[⊥], **Shih-Sheng Sun**[⊥], **Yang Yang**[‖], **Hsiao-hua Yu**[⊥], **Kai Chen**[§], **Gary S. Chuang**[¶], and **Hsian-Rong Tseng**[†,iD]

[†]Department of Molecular and Medical Pharmacology, Crump Institute for Molecular Imaging (CIMI), California NanoSystems Institute (CNSI), Institute for Molecular Medicine (IMED), University of California, Los Angeles, California 90095-1770, United States

[‡]Department of Pathology, Guangdong Provincial Hospital of TCM, Guangzhou University of Chinese Medicine, Guangzhou 510405, China

[§]Molecular Imaging Center, Department of Radiology, Keck School of Medicine, University of Southern California, Los Angeles, California 90033-9061, United States

[⊥]Institute of Chemistry, Academia Sinica, Nangang, Taipei 115, Taiwan, R.O.C

[‖]Department of Materials Science and Engineering, California NanoSystems Institute (CNSI), University of California, Los Angeles, California 90095, United States

[¶]Division of Dermatology, David Geffen School of Medicine at UCLA, Los Angeles, California 90095, United States

Abstract

Tattooing has been utilized by the medical community for precisely demarcating anatomic landmarks. This practice is especially important for identifying biopsy sites of nonmelanoma skin cancer (NMSC) due to the long interval (*i.e.*, up to 3 months) between the initial diagnostic biopsy and surgical treatment. Commercially available tattoo pigments possess several issues, which include causing poor cosmesis, being mistaken for a melanocytic lesion, requiring additional removal procedures when no longer desired, and potentially inducing inflammatory responses. The ideal tattoo pigment for labeling of skin biopsy sites for NMSC requires (i) invisibility under ambient light, (ii) fluorescence under a selective light source, (iii) a finite intradermal retention

Correspondence to: Kai Chen; Gary S. Chuang; Hsian-Rong Tseng.

ORCID

Hsian-Rong Tseng: 0000-0001-9028-8527

ASSOCIATED CONTENT

Supporting Information

The Supporting Information is available free of charge on the ACS Publications website at DOI: 10.1021/acsnano.6b06200. Preparation of FSNPs with various sizes by changing the Ad-PAMAM/CD-PEI ratio (w/w), absorption spectra of FSNPs with various Ad-PAMAM/CD-PEI ratios (w/w), tattooing with commercially available tattoo dyes, pathological study of commercially available tattoo dyes (PDF)

The authors declare no competing financial interest.

time (*ca.* 3 months), and (iv) biocompatibility. Herein, we introduce cross-linked fluorescent supra-molecular nanoparticles (*c*-FSNPs) as a “finite tattoo” pigment, with optimized photophysical properties and intradermal retention time to achieve successful *in vivo* finite tattooing. Fluorescent supramolecular nanoparticles encapsulate a fluorescent conjugated polymer, poly[5-methoxy-2-(3-sulfopropoxy)-1,4-phenylenevinylene] (MPS-PPV), into a core *via* a supramolecular synthetic approach. FSNPs which possess fluorescent properties superior to those of the free MPS-PPV are obtained through a combinatorial screening process. Covalent cross-linking of FSNPs results in micrometer-sized *c*-FSNPs, which exhibit a size-dependent intradermal retention. The 1456 nm sized c-FSNPs display an ideal intradermal retention time (*ca.* 3 months) for NMSC lesion labeling, as observed in an *in vivo* tattoo study. In addition, the *c*-FSNPs induce undetectable inflammatory responses after tattooing. We believe that the c-FSNPs can serve as a “finite tattoo” pigment to label potential malignant NMSC lesions.

Graphical Abstract

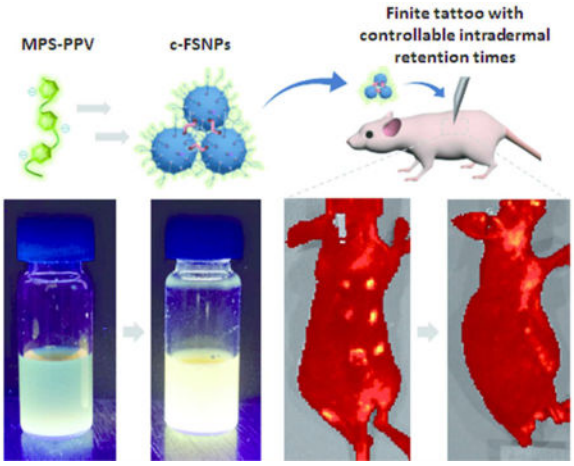

Keywords

supramolecular nanoparticles; finite tattoo; fluorescent conjugated polymer; cross-linking; controllable intradermal retention time

In recent decades of increased sun exposure, over 3.3 million cases of nonmelanoma skin cancers (NMSCs) are diagnosed each year, rising at a faster rate than breast, prostate, lung, and colon cancers combined.[1] In routine clinical practice, a suspected NMSC lesion is diagnosed *via* histologic characterization of biopsied skin tissues. Once the biopsy is confirmed to be a NMSC, the patient is then scheduled for a definitive treatment, which includes electrodessication, cryotherapy, topical chemotherapy, immune modulation, surgical excision, or Mohs micrographic surgery. Since the time interval between the initial diagnostic biopsy and the scheduled surgical treatment can last up to 3 months, depending on availability of treatment,[2] the biopsy site can recover remarkably well and thus become nearly invisible for a physician to identify. Besides photographic and pictorial documentation,[3–5] labeling a potential NMSC lesion with a “tattoo”, a form of dermal pigmentation, is an approach that can effectively identify the biopsy site of NMSC lesion for

the treatment.[6–8] There are two major types of tattoo pigments in clinical use but with significant limitations: (i) conventional carbon graphite and India ink,[6] which are cosmetically unappealing and may be mistaken for a melanocytic lesion, and (ii) fluorescent particles (e.g., ZnO or dye-doped poly(methyl methacrylate) (PMMA) particles),[7,8] which can only be visualized under UV light. To permanently remove these long-lasting fluorescent tattoo marks,[9,10] laser or surgical treatments are often needed. In addition, both tattoo pigments may cause local inflammatory responses (*e.g.*, dermatitis), leading to discomfort at the tattoo sites.[11,12] Ideal tattoo pigments for short-term labeling of potential NMSC lesions require (i) invisibility under ambient visible light, (ii) fluorescent properties for detection under a given light source, (iii) a finite intradermal retention time of approximately 3 months, and (iv) biocompatibility to prevent any irritation at or around the tattoo sites.

Herein, we introduce a finite fluorescent tattoo pigment, cross-linked fluorescent supramolecular nanoparticles (c-FSNPs). We demonstrated that these c-FSNPs exhibit enhanced photophysical properties, a finite intradermal retention, and biocompatibility, making them a promising candidate as an ideal tattoo pigment for short-term labeling of potential NMSC lesions. To prepare c-FSNPs with desired photophysical and *in vivo* properties, we first synthesized fluorescent supramolecular nanoparticles (FSNPs), with enhanced fluorescent properties, by encapsulating a fluorescent conjugated polymer, poly[5-methoxy-2-(3-sulfopropoxy)-1,4-phenylenevinylene] (MPS-PPV), into the intraparticular space of supramolecular nanoparticles (SNP) via a supramolecular synthetic approach[13–25] (Figure 1a). By altering the synthetic parameters (*i.e.*, ratios among MPS-PPV and the molecular building blocks), differential photophysical properties can be programmed into a small combinatorial library of FSNPs. We found 670 nm sized FSNPs to exhibit an optimal fluorescent performance with 10-fold enhancement compared that of free MPS-PPV. Furthermore, we conducted a cross-linking reaction on 670 nm sized FSNPs to generate micrometer-sized c-FSNPs, which have a size-dependent and finite intradermal retention time (Figure 1b,c). In this study, we successfully performed short-term labeling using c-FSNPs, which are invisible under ambient light but retain their fluorescent signal up to *ca.* 3 months (Figure 1c). Furthermore, an *in vivo* study reveals that the c-FSNPs induce undetectable local inflammatory responses, which are commonly triggered by commercially available tattoo pigments.

RESULTS AND DISCUSSION

We employed a supramolecular synthetic approach[13–25] to prepare FSNPs, which encapsulate MPS-PPV (0.005–0.15 mg/ mL) into a SNP core, from three molecular building blocks, that is, cationic adamantane (Ad)-grafted polyamidoamine dendrimer (Ad-PAMAM; 0.15–1.6 mg/mL), cationic β-cyclodextrin (CD)-grafted branched polyethylenimine (CD-PEI; 0.8 mg/mL), and Ad-grafted polyethylene glycol (Ad-PEG; 1.836 mg/mL) (Figure 2a and Supporting Information Figure S1). Given the fact that the intraparticular space of SNPs is composed of a cationic Ad-PAMAM/CD-PEI hydrogel network, it is conceivable that FSNPs can encapsulate anionic MPS-PPV *via* electrostatic interactions.[14,15,26,27] FSNPs with optimal fluorescent performance were identified through a combinatorial screening process. A small combinatorial library composed of 27 different formulations of FSNPs was

prepared by changing the ratios among the molecular building blocks: (i) MPS-PPV/CD-PEI ratios (w/w; 0.006:1, 0.016:1, 0.031:1, 0.125:1, and 0.186:1) and (ii) Ad-PAMAM/CD-PEI ratios (w/ w; 0.19:1, 0.25:1, 0.5:1, 1.0:1, 1.5:1, 1.7:1, and 2.0:1). The fluorescent intensities of the resulting FSNPs were measured with a fluorometer and normalized to the observed intensities of free MPS-PPV at corresponding concentrations for each FSNP formulation. A three-dimensional profile summarizes the normalized fluorescent intensities of the resulting FSNPs (Figure 2b). The FSNPs exhibiting optimal fluorescent performance (⋆), where FSNPs possess the highest normalized fluorescent intensities with the largest MPS-PPV loading in the core, were obtained with a specific formulation of the mixing ratio among the molecular building blocks, that is, MPS-PPV/CD-PEI ratio (w/w) = 0.125:1 and Ad-PAMAM/ CDPEI ratio (w/w) = 2.0:1.

FSNPs with the optimal fluorescent performance, identified from the combinatorial library (Figure 2b, ⋆), were then subjected to (i) characterization of their structural and photophysical properties and (ii) cluster formation studies via a cross-linking process. As shown in Figure 3a, the hydrodynamic size, obtained by dynamic light scattering (DLS), of the FSNPs prepared by the optimal condition as described above was 670 ± 43 nm, and their morphology observed in transmission electron microscopic (TEM) image reveals homogeneous spherical nanoparticles (Figure 3b). The size of FSNPs in TEM images was measured as 498 ± 37 nm, which is smaller than the hydrodynamic size obtained by DLS due to dehydration of FSNPs during the sample preparation for TEM imaging.

Under UV light irradiation, the 670 nm sized FSNPs displayed dramatically enhanced fluorescence compared to that of the free MPS-PPV aqueous solution. The difference in their fluorescent performance was so dramatic that it was easily distinguished with the naked eye (Figure 3c). Comparison of the fluorescence spectra confirmed that the emission of 670 nm sized FSNP was ca. 10-fold greater than that of free MPS-PPV (Figure 3d). FSNPs possessed a broad absorption band (maximum absorption peak at 440 nm), where FSNPs exhibit *ca.* 6.8 times higher absorption than free MPS-PPV (Figure 3e and Supporting Information Figure S2). Analysis of the absorption and fluorescence spectra of 670 nm sized FSNPs indicated an absorption cross section of 1.17×10^{-16} cm^{-2} and quantum yield (QY) of 4%. In contrast, free MPS-PPV showed a smaller absorption cross section of 1.72×10^{-17} cm^{-2} and a lower QY of 0.45% (Figure 3f). The enhanced fluorescence in our FSNPs is most likely due to the aggregation disassembly through the electrostatic interactions with CD-PEI. Bare MPS-PPV chains coiled and formed face-to-face π-stacking among phenyl rings.[28] Therefore, the fluorescence is highly quenched. Once CD-PEI is introduced in the FSNPs, they form a complex with MPS-PPV polymer chains electrostatically, separating and uncoiling individual polymer chains. This was supported by the blue-shifted emission in FSNPs (MPS-PPV = 520 nm *vs* FSNP = 507 nm).[28–30] In addition, uncoiling of MPS-PPV reduced the conformational disorder (*e.g.*, kink defects) of the polymer, resulting in a decrease of nonradiative decay (*e.g.*, see fluorescent lifetime in Figure 3f; MPS-PPV = 0.55 and 2.11 ns *vs* FSNPs = 0.78 and 2.08 ns) and enhancement of QY.[31,32] Increase in absorption cross section also supported the rationale mentioned above. Aggregation of π-conjugated systems often resulted in the decrease of UV–visible light absorption.[33,34] Therefore, the absorption cross section should increase when polymer aggregations were disassembled in FSNPs.

In previous studies, conjugated polymer-based nanoparticles have generally required multiple optimization cycles of design and modification of the molecular structures of the core-conjugated polymer[35–38] to reach the best optical performance. In contrast, FSNPs with optimal fluorescent properties can be selected from a combinatorial library in which different formulations of FSNPs were readily prepared by changing the ratios among MPS-PPV and the three molecular building blocks via our flexible and convenient supramolecular synthetic approach. By controlling the ratio of assembling building blocks, the composition of FSNPs could be easily tuned and those with optimal fluorescent properties could be readily obtained. For example, enhanced fluorescent properties of FSNPs were obtained by increasing the Ad-PAMAM/CD-PEI ratio,[13] which was supported by the increased absorption of FSNPs (Supporting Information Figures S1 and S2). On the other hand, a high concentration of MPS-PPV in the FSNP core would lead to aggregation-caused quenching.[39] Therefore, an optimized MPS-PPV/CD-PEI ratio (≤0.125, Figure 2b) was screened and obtained, reducing the interchain interaction among MPS-PPVs in FSNPs. Our supramolecular synthetic approach is capable of rapid and parallel programming of a combinatorial library of FSNPs and provides a developmental pathway to overcome the limitation of the conventional time-and cost-consuming optimization process in search of ideal fluorescent nanoparticles.

After identification of the 670 nm sized FSNPs with optimal fluorescent performance, we studied the correlation between size and the intradermal retention time of FSNPs. The commercially available fluorescent tattoo pigments (*e.g.*, ZnO, fluorescent dye-doped PMMA, and India ink), which possess a permanent intradermal retention time, have a size of one to several micrometers, as observed from TEM studies (Supporting Information Figure S3a–c). Based on the dimensions of these commercially available tattoo pigments, we tested the intradermal retention time of FSNPs with sizes ranging from hundreds of nanometers to a few micrometers. We were able to obtain a collection of FSNPs with controllable sizes up to 670 nm by using the supramolecular synthetic approach (Supporting Information Figure S1). In order to construct micrometersized particles, we applied a covalent cross-linker bis-(sulfosuccinimidyl)suberate (BS3, 1–3 μg/mL) to “glue” several 670 nm FSNPs to form micrometer-sized c-FSNPs (Figure 4a). BS3 reacts with the free amine groups in the FSNPs, leading to both intra- and inter-FSNP cross-linking reactions. Inter-FSNP cross-linking resulted in the formation of various-sized c-FSNPs, whose sizes depended on the concentration of BS3. By controlling the quantity of the cross-linker, we successfully produced c-FSNPs with sizes up to 1456 nm. The hydrodynamic size of c-FSNPs increased from 679 ± 51 nm to 884 ± 62 and 1456 ± 110 nm when 1, 2, and 3 μg/mL of BS3 was introduced to the 670 nm sized FSNP solution, respectively (Figure 4b – e). TEM analysis confirmed that c-FSNP is composed of 670 nm sized FSNPs, which are cross-linked interparticularly, maintaining their size and morphology.

We then examined the intradermal retention times of 679, 884, and 1456 nm sized c-FSNPs along with 240, 410, and 670 nm sized FSNPs. These c-FSNPs and FSNPs were tattooed at six different locations on the back of nu/nu mice (n = 3) (Figure 5a). Following a typical tattooing protocol, FSNPs and c-FSNPs, each containing 0.75 μg of MPS-PPV, were deposited in the dermis through wounds generated by poking with a needle (Figure 1b). The deposited FSNPs and c-FSNPs stayed in the dermis after the wounds healed. After tattooing,

no visible signal from FSNPs and c-FSNPs was observed under ambient light irradiation, as shown in Figure 5b. The fluorescent signals from these tattooed FSNPs and c-FSNPs were obtained up to 94 days using an *in vivo* optical imaging system (excitation/emission = 465/520 nm, exposure time = 2 s; Figure 5c). The time-dependent fluorescent signals of FSNPs and c-FSNPs are summarized in Figure 5d, where fluorescent signals are normalized to the initial fluorescent signal intensity at day 0. The tattooed FSNPs and c-FSNPs exhibit a size-dependent intradermal retention time (Figure 5c,d). Longer intradermal retention times can be obtained with the larger-sized particles. As a result, 1456 nm sized c-FSNPs (white arrow in Figure 5c) show the slowest fluorescent signal decay and maintain their fluorescent signal up to 84 days (12 weeks, *ca.* 3 months). At day 94, all fluorescent signals from the tattooed FSNPs and c-FSNPs diminished to undetectable levels. In contrast, the commercially available tattoo pigment (*i.e.*, ZnO, *ca.* 5 μm) exhibited a consistent fluorescent intensity over 94 days (Figure 5d and Supporting Information Figure S3d).

The size of c-FSNPs plays an important role in modulating their intradermal retention time. Moreover, it is noteworthy that 670 nm sized FSNPs exhibit a fast fluorescent signal drop in a week while 679 nm sized c-FSNPs with a similar size show a gradual fluorescent signal decrease over 8 weeks (56 days). It is clear that the covalent intra-FSNP cross-linking plays an important role in delaying the dynamic disassembly of c-FSNPs by tightening the structure of FSNPs. The dynamic nature of the Ad-CD self-assembly motifs,[14,40] employed in the preparation of our FSNPs, leads to disassembly of FSNPs under physiological conditions. This disassembly rate is too fast to satisfy the current needs for the “finite tattoo” in the animal study with the 670 nm sized FSNPs. The additional intraparticular cross-linking in c-FSNPs is thus necessary to delay this disassembly process so that the intradermal retention time of 679 nm sized c-FSNPs is elongated compared to that of 670 nm sized FSNPs. Overall, the intradermal retention time of c-FSNPs is governed by both their size and cross-linking.

A pathological study of animal skin was conducted at 2 days after tattooing to validate the biocompatibility of c-FSNPs. In the H&E [hematoxylin (nucleus staining) and eosin (cytoplasm staining)] stained tissue sections, no obvious inflammatory cells were observed after c-FSNP tattooing compared to normal skin (Figure 5e(i,ii)). In contrast, commercially available tattoo pigments (*i.e.*, ZnO and PMMA) attract a large population of inflammation cells, such as lymphocytes, after tattooing (Figure 5e(iii) and Supporting Information Figure S4). Because c-FSNPs are composed of molecular building blocks (*e.g.*, CD, PEG) which are known to be nonimmunogenic,[41–43] they exhibit biocompatibility without inducing any inflammatory reactions at or around the tattoo sites.

CONCLUSIONS

We have developed a finite tattoo pigment, c-FSNPs, with strong fluorescent properties, a controllable lifetime, and biocompatibility to achieve successful *in vivo* finite tattooing. The 670 nm sized FSNPs with optimal fluorescent properties selected *via* a combinatorial screening process were cross-linked to form micrometer-sized c-FSNPs. c-FSNPs provide a fluorescent signal in the skin under 465 nm light excitation without being cosmetically unappealing under ambient light irradiation. Unlike commercially available tattoo pigments

with permanent intradermal retention, c-FSNPs are clearable but with an appropriate intradermal retention time in the skin. The retention time of c-FSNPs can be modulated by controlling the size and cross-linking chemistry. c-FSNPs with a 1456 nm hydrodynamic size show an intradermal retention time of up to 84 days (12 weeks, 3 months), which matches the typical period between biopsy and treatment in the clinic. In addition, c-FSNPs are biocompatible and do not induce any dermal inflammatory reactions. We believe that our c-FSNPs can serve as a “finite tattoo” pigment to label potential malignant NMSC lesions. The translation of our c-FSNPs into NMSC patients is underway with the hope of providing the correct information on the biopsied potential malignant sites.

MATERIALS AND METHODS

Materials

Reagents and solvents were used as received without further purification unless otherwise noted. Branched polyethylenimine (PEI, MW = 10 kDa) was purchased from Polysciences Inc. (Washington, PA). Polymers contain primary, secondary, and tertiary amine groups in a ratio of approximately 25/50/25. First-generation polyamidoamine dendrimer (PAMAM) with a 1,4-diaminobutane core and amine terminals in 20 wt % methanol solution was purchased from Dendritic Nanotechnologies, Inc. (Mount Pleasant, MI). 1-Adamantanamine (Ad) hydrochloride and β-cyclodextrin (β-CD) were purchased from TCI America (San Francisco, CA). N-Hydroxysuccinimide (SCM) and maleimido (MAL) heterofunctionalized polyethylene glycol (SCM-PEG-MAL, MW = 5 kDa) were obtained from NANOCS Inc. (New York, NY). 6-Monotosyl-β-cyclodextrin (6-OTs-β-CD) was prepared according to the literature reported method.[44] Octa-Ad-grafted polyamidoamine dendrimer (Ad-PAMAM), CD-grafted branched polyethylenimine (CD-PEI), and Ad-grafted polyethylene glycol (Ad-PEG) were prepared by the method we previously reported.[13] Poly[5-methoxy-2-(3-sulfopropoxy)-1,4-phenylenevinylene]potassium salt (MPS-PPV) was purchased from Aldrich (St. Louis, MO). The hydrodynamic size of FSNPs and c-FSNPs was measured on a Zetasizer Nano instrument (Malvern Instruments Ltd., United Kingdom). Transmission electron microscope images of FSNPs and c-FSNPs were taken with a Philips CM 120 electron microscope operating with an acceleration voltage of 120 kV. PL measurements were conducted with a HORIBA Jobin Yvon system (Horiba, Japan), and the UV–vis absorption spectrum was obtained with the Hitachi UV–vis system (Hitachi U-4100 spectrophotometer, Hitachi, Japan). *In vivo* fluorescent images were obtained with the IVIS-200 optical imaging system (PerkinElmer, Waltham, MA). Pathological images of tissue sample after tattooing were obtained with the Aperio ScanScope AT microscope (Leica Biosystem, USA).

Preparation of FSNPs

To a solution of Ad-PEG (1.836 mg/mL) in 485 μL of PBS buffer, CD-PEI (0.8 mg/mL), was injected CD-PEI (0.8 mg/mL) under vigorous stirring. MPS-PPV (0.005–0.15 mg/ mL) was then added sequentially, and the mixture solution was stirred vigorously for 2 min. A 5 μL aliquot of dimethylsulfoxide containing Ad-PAMAM (0.15–1.6 mg/mL) was added into the mixture solution to obtain FSNPs.

Characterization Methods and Settings

Dynamic Light Scattering—The hydrodynamic sizes of FSNPs and c-FSNPs were measured with a Zetasizer Nano instrument (Malvern Instruments Ltd., United Kingdom) equipped with a 10 mW helium–neon laser (λ = 632.8 nm) and a thermoelectric temperature controller. Measurements were taken at a 90° scattering angle. The hydrodynamic sizes of FSNPs and c-FSNPs were obtained by averaging the values of three or more measurements.

Transmission Electron Microscopy—The morphology and sizes of FSNPs and c-FSNPs were examined using a TEM. The studies were carried out on a Philips CM 120 electron microscope, operating at an acceleration voltage of 120 kV. TEM samples were prepared by dropcoating 2 μL of sample suspension solutions onto carbon-coated copper grids. Excess amounts of solution were removed by filter papers after 45 s. Subsequently, the samples were negatively stained with 2% uranyl acetate for 45 s before TEM studies.

Photoluminescence—Steady-state photoluminescence (PL) of free MPS-PPV and FSNPs was measured using a custom-made PL system (HORIBA Jobin Yvon system, Horiba, Japan). The solutions of FSNPs and MPS-PPV were excited by a xenon lamp, which filtered its wavelength using a monochromator with a wavelength of 450 nm.

UV–Vis Absorption—The UV–vis absorption of free MPS-PPV and FSNPs was obtained with a Hitachi UV–vis system (Hitachi U-4100 spectrophotometer, Hitachi, Japan). The absorption of free MPS-PPV and FSNPs was obtained from 350 to 800 nm with a scan speed of 10 nm/s with 1 nm intervals.

Fluorescent Lifetime Measurement—Time-correlated single-photon counting (TCSPC) was used to determine the lifetime of free MPS-PPV and FSNPs. In TCSPC, each sample was measured with time between sample excitation by a pulse of laser and the arrival of the emitted photons to the detector. The measured lifetime spectrum was then fitted by an exponential fit time scan to get the fitting curve and lifetime data. All the data were obtained three times on an Edinburgh FLS920 time-correlated single-photon-counting instrument. Samples were excited at 475 nm from a picosecond diode laser with 90 ps pulse width transmitted through a Czerny-Turner design monochromator. The emission wavelength can be detected at 90° *via* a second Czerny-Turner design monochromator onto a MCP-PMT with a response time down to 25 ps. The instrument response function was profiled using a scatter solution and subsequently deconvoluted from the emission data to yield an undisturbed decay. Nonlinear least-squares fitting of the decay curves was performed with the Levenberg–Marquardt algorithm and implemented by the Edinburgh Instruments FAST software.

Calculation of Absorption Cross Section

The absorption cross section of free MPS-PPV and FSNPs was calculated from the mass absorption coefficient[45] using

$$\sigma = \frac{2.303(1000)\varepsilon}{N_A} (\mathrm{cm}^2/\mathrm{polymer\ \ unit})$$

where ε is the stated molar extinction coefficient (M^{-1} cm^{-1}) and N_A is Avogadro's number. The factor of 1000 originates from a conversion between dm^3 and cm^3 , and 1/log e = 2.303.

Calculation of Fluorescent Quantum Yield

The relative QY of free MPS-PPV and FSNPs was determined by comparison with a fluorophore (Cy3) of known QY with the same experimental parameters as free MPS-PPV and FSNPs.

The QY was calculated by

$$\Phi = \Phi_R \times \frac{\mathrm{Int}}{\mathrm{Int}_R} \frac{1 - 10^{-A_R}}{1 - 10^{-A}} \frac{n^2}{{n_R}^2}$$

where Φ is the QY, Int is the area under the emission peak, A is absorbance at the excitation wavelength, and n is the refractive index of the solvent. The subscript R denotes the respective values of the reference substance, Cy3 (Lumiphore, Hallandale Beach, FL, USA; QY = 0.31).

Preparation of c-FSNPs

The 670 nm sized FSNPs were mixed with various concentrations of BS3 from 1 to 2 and 3 μg/mL at room temperature with vigorous stirring. After 15 min, Tris buffer (1×) was added to the reaction solution in order to stop the cross-linking reaction of BS3.

Examination on Intradermal Retention Time of c-FSNPs

All animal manipulations were performed with sterile techniques and were approved by the Institutional Animal Care and Use Committee of University of Southern California. Female athymic nude mice (about 6–8 weeks old, with a body weight of 20–25 g) were purchased from Envigo (Livermore, CA, USA). The FSNPs and c-FSNPs were tattooed at six different locations on the back of nu/nu mice (n = 3), following the typical tattooing protocol. After the mice were anesthetized with 2% isoflurane in a heated (37 °C) induction chamber, mouse skin was poked with a 25 G needle to make wounds to the dermis layer. FSNP or c-FSNP solution was dropped on the wounded mouse skin (nu/nu) to deposit FSNP or c-FSNP into the dermis layer through the wounds. The FSNP or c-FSNP solution was washed away with saline several times. After tattooing, the signals of FSNP and c-FSNP were measured with the *in vivo* optical imaging system (IVIS-200, PerkinElmer, Waltham, MA, USA) for 94 days.

Pathological Studies of Skin Tissues Tattooed with c-FSNPs

Another group of mice, treated the same as described above in the *in vivo* study, had their skin tissues taken 2 days after tattooing for pathological studies. Skin tissues were fixed with

10% formalin and blocked with paraffin, following conventional laboratory methods. Slices of skin tissue were stained with H&E solution for pathological study. Tissues were then examined using an Aperio ScanScope AT microscope (Leica biosystem, USA). Each H&E stained tissue slide was evaluated by two independent pathologists.

Supplementary Material

Refer to Web version on PubMed Central for supplementary material.

Acknowledgments

This research was supported by the National Institutes of Health (R21EB016270) and the Department of Radiology at USC.

References

1. Rogers HW, Weinstock MA, Feldman SR, Coldiron BM. Incidence Estimate of Nonmelanoma Skin Cancer (Keratinocyte Carcinomas) in the US Population, 2012. JAMA Dermatol. 2015; 151:1081–1086. [PubMed: 25928283]
2. Kimball AB, Resneck JS. The US Dermatology Workforce: A Specialty Remains in Shortage. J. Am. Acad. Dermatol. 2008; 59:741–745. [PubMed: 18723242]
3. Campbell RM, Perlis CS, Malik MK, Dufresne RG. Characteristics of Mohs Practices in the United States: A Recall Survey of Acms Surgeons. Dermatol. Surg. 2007; 33:1413–1418. [PubMed: 18076605]
4. McGinness JL, Goldstein G. The Value of Preoperative Biopsysite Photography for Identifying Cutaneous Lesions. Dermatol. Surg. 2010; 36:194–197. [PubMed: 20039919]
5. Ke M, Moul D, Camouse M, Avram M, Carranza D, Soriano T, Lask G. Where Is It? The Utility of Biopsy-Site Photography. Dermatol. Surg. 2010; 36:198–202. [PubMed: 20039920]
6. Laumann AE, Derick AJ. Tattoos and Body Piercings in the United States: A National Data Set. J. Am. Acad. Dermatol. 2006; 55:413–421. [PubMed: 16908345]
7. Chuang GS, Gilchrest BA. Ultraviolet-Fluorescent Tattoo Location of Cutaneous Biopsy Site. Dermatol. Surg. 2012; 38:479–483. [PubMed: 22171575]
8. Russell K, Schleichert R, Baum B, Villacorta M, Hardigan P, Thomas J, Weiss E. Ultraviolet-Fluorescent Tattoo Facilitates Accurate Identification of Biopsy Sites. Dermatol. Surg. 2015; 41:1249–1256. [PubMed: 26445291]
9. Bondarenko O, Juganson K, Ivask A, Kasemets K, Mortimer M, Kahru A. Toxicity of Ag, CuO and ZnO Nanoparticles to Selected Environmentally Relevant Test Organisms and Mammalian Cells in Vitro: A Critical Review. Arch. Toxicol. 2013; 87:1181–1200. [PubMed: 23728526]
10. Zhang Z-Y, Xiong H-M. Photoluminescent ZnO Nano-particles and Their Biological Applications. Materials. 2015; 8:3101–3127.
11. Cook J, Metcalf J. Tattoo Allergy. N. Engl. J. Med. 2009; 361:e1. [PubMed: 19571278]
12. Wenzel SM, Rittmann I, Landthaler M, Baumler W. Adverse Reactions after Tattooing: Review of the Literature and Comparison to Results of a Survey. Dermatology. 2013; 226:138–147. [PubMed: 23689478]
13. Wang H, Wang S, Su H, Chen KJ, Armijo AL, Lin WY, Wang Y, Sun J, Kamei K, Czernin J, Radu CG, Tseng HR. A Supramolecular Approach for Preparation of Size-Controlled Nanoparticles. Angew. Chem., Int. Ed. 2009; 48:4344–4348.
14. Wang H, Liu K, Chen KJ, Lu Y, Wang S, Lin WY, Guo F, Kamei K, Chen YC, Ohashi M, Wang M, Garcia MA, Zhao XZ, Shen CK, Tseng HR. A Rapid Pathway toward a Superb Gene Delivery System: Programming Structural and Functional Diversity into a Supramolecular Nanoparticle Library. ACS Nano. 2010; 4:6235–6243. [PubMed: 20925389]

15. Wang H, Chen KJ, Wang S, Ohashi M, Kamei K, Sun J, Ha JH, Liu K, Tseng HR. A Small Library of DNA-Encapsulated Supramolecular Nanoparticles for Targeted Gene Delivery. Chem. Commun. 2010; 46:1851–1853.
16. Stoffelen C, Voskuhl J, Jonkheijm P, Huskens J. Dual Stimuli-Responsive Self-Assembled Supramolecular Nanoparticles. Angew. Chem., Int. Ed. 2014; 53:3400–3404.
17. Stoffelen C, Huskens J. Size-Tunable Supramolecular Nanoparticles Mediated by Ternary Cucurbit[8]Uril Host-Guest Interactions. Chem. Commun. 2013; 49:6740–6742.
18. Tonga GY, Mizuhara T, Saha K, Jiang Z, Hou S, Das R, Rotello VM. Binding Studies of Cucurbit[7]Uril with Gold Nanoparticles Bearing Different Surface Functionalitie. Tetrahedron Lett. 2015; 56:3653–3657. [PubMed: 26074630]
19. Kim C, Tonga GY, Yan B, Kim CS, Kim ST, Park M-H, Zhu Z, Duncan B, Creran B, Rotello VM. Regulating Exocytosis of Nanoparticles *via* Host-Guest Chemistry. Org. Biomol. Chem. 2015; 13:2474–2479. [PubMed: 25569869]
20. Cabral H, Nishiyama N, Kataoka K. Supramolecular Nanodevices: From Design Validation to Theranostic Nanomedicine. Acc. Chem. Res. 2011; 44:999–1008. [PubMed: 21755933]
21. Fukushima K, Liu S, Wu H, Engler AC, Coady DJ, Maune H, Pitera J, Nelson A, Wiradharma N, Venkataraman S, Huang Y, Fan W, Ying JY, Yang YY, Hedrick JL. Supramolecular High-Aspect Ratio Assemblies with Strong Antifungal Activity. Nat. Commun. 2013; 4:2861. [PubMed: 24316819]
22. Lee J-H, Chen K-J, Noh S-H, Garcia MA, Wang H, Lin W-Y, Jeong H, Kong BJ, Stout DB, Cheon J, Tseng H-R. On-Demand Drug Release System for *in Vivo* Cancer Treatment through Self-Assembled Magnetic Nanoparticles. Angew. Chem., Int. Ed. 2013; 52:4384–4388.
23. Wang S, Chen KJ, Wu TH, Wang H, Lin WY, Ohashi M, Chiou PY, Tseng HR. Photothermal Effects of Supramolecularly Assembled Gold Nanoparticles for the Targeted Treatment of Cancer Cells. Angew. Chem., Int. Ed. 2010; 49:3777–3781.
24. Chen KJ, Wolahan SM, Wang H, Hsu CH, Chang HW, Durazo A, Hwang LP, Garcia MA, Jiang ZK, Wu L, Lin YY, Tseng HR. A Small MRI Contrast Agent Library of Gadolinium(III)-Encapsulated Supramolecular Nanoparticles for Improved Relaxivity and Sensitivity. Biomaterials. 2011; 32:2160–2165. [PubMed: 21167594]
25. Chen KJ, Tang L, Garcia MA, Wang H, Lu H, Lin WY, Hou S, Yin Q, Shen CK, Cheng J, Tseng HR. The Therapeutic Efficacy of Camptothecin-Encapsulated Supramolecular Nanoparticles. Biomaterials. 2012; 33:1162–1169. [PubMed: 22074663]
26. Liu Y, Wang H, Kamei K, Yan M, Chen KJ, Yuan Q, Shi L, Lu Y, Tseng HR. Delivery of Intact Transcription Factor by Using Self-Assembled Supramolecular Nanoparticles. Angew. Chem. Int. Ed. 2011; 50:3058–3062.
27. Yin L, Song Z, Kim KH, Zheng N, Gabrielson NP, Cheng J. Non-Viral Gene Delivery *via* Membrane-Penetrating, Mannose-Targeting Supramolecular Self-Assembled Nanocomplexes. Adv. Mater. 2013; 25:3063–3070. [PubMed: 23417835]
28. Ng BC, Chan ST, Lin J, Tolbert SH. Using Polymer Conformation to Control Architecture in Semiconducting Polymer/ Viral Capsid Assemblies. ACS Nano. 2011; 5:7730–7738. [PubMed: 21942298]
29. Tan C, Pinto MR, Schanze KS. Photophysics, Aggregation and Amplified Quenching of a Water-Soluble Poly(Phenylene Ethynylene). Chem. Commun. 2002:446–447.
30. Chen L, Xu S, McBranch D, Whitten D. Tuning the Properties of Conjugated Polyelectrolytes through Surfactant Complexation. J. Am. Chem. Soc. 2000; 122:9302–9303.
31. Dimitrov SD, Schroeder BC, Nielsen CB, Bronstein H, Fei Z, McCulloch I, Heeney M, Durrant JR. Singlet Exciton Lifetimes in Conjugated Polymer Films for Organic Solar Cells. Polymers. 2016; 8:14.
32. Cadby AJ, Dean R, Elliott C, Jones RAL, Fox AM, Lidzey DG. Imaging the Fluorescence Decay Lifetime of a Conjugated-Polymer Blend by Using a Scanning near-Field Optical Microscope. Adv. Mater. 2007; 19:107–111.
33. Rao MR, Liao C-W, Sun S-S. Structurally Simple Thienodipyrandione-Containing Reversible Fluorescent Switching Piezo- and Acidochromic Materials. J. Mater. Chem. C. 2013; 1:6386–6394.

34. Peyratout C, Daehne L. Aggregation of Thiacyanine Derivatives on Polyelectrolytes. Phys. Chem. Chem. Phys. 2002; 4:3032–3039.
35. Wu C, Bull B, Szymanski C, Christensen K, McNeill J. Multicolor Conjugated Polymer Dots for Biological Fluorescence Imaging. ACS Nano. 2008; 2:2415–2423. [PubMed: 19206410]
36. Wu C, Chiu DT. Highly Fluorescent Semiconducting Polymer Dots for Biology and Medicine. Angew. Chem., Int. Ed. 2013; 52:3086–3109.
37. Li K, Liu B. Polymer-Encapsulated Organic Nanoparticles for Fluorescence and Photoacoustic Imaging. Chem. Soc. Rev. 2014; 43:6570–6597. [PubMed: 24792930]
38. Wu C, Schneider T, Zeigler M, Yu J, Schiro PG, Burnham DR, McNeill JD, Chiu DT. Bioconjugation of Ultrabright Semiconducting Polymer Dots for Specific Cellular Targeting. J. Am. Chem. Soc. 2010; 132:15410–15417. [PubMed: 20929226]
39. Ma X, Sun R, Cheng J, Liu J, Gou F, Xiang H, Zhou X. Fluorescence Aggregation-Caused Quenching *versus* Aggregation-induced Emission: A Visual Teaching Technology for Undergraduate Chemistry Students. J. Chem. Educ. 2016; 93:345–350.
40. Hou S, Choi J-s, Garcia MA, Xing Y, Chen K-J, Chen Y-M, Jiang ZK, Ro T, Wu L, Stout DB, Tomlinson JS, Wang H, Chen K, Tseng H-R, Lin W-Y. Pretargeted Positron Emission Tomography Imaging That Employs Supramolecular Nanoparticles with *in Vivo* Bioorthogonal Chemistry. ACS Nano. 2016; 10:1417–1424. [PubMed: 26731174]
41. Schellekens H, Hennink WE, Brinks V. The Immunogenicity of Polyethylene Glycol: Facts and Fiction. Pharm. Res. 2013; 30:1729–1734. [PubMed: 23673554]
42. Ganson NJ, Kelly SJ, Scarlett E, Sundy JS, Hershfield MS. Control of Hyperuricemia in Subjects with Refractory Gout, and Induction of Antibody against Poly(Ethylene Glycol) (PEG), in a Phase I Trial of Subcutaneous PEGylated Urate Oxidase. Arthritis Res. Ther. 2006; 8:R12. [PubMed: 16356199]
43. Veronese FM, Pasut G. Pegylation, Successful Approach to Drug Delivery. Drug Discovery Today. 2005; 10:1451–1458. [PubMed: 16243265]
44. Petter RC, Salek JS, Sikorski CT, Kumaravel G, Lin FT. Cooperative Binding by Aggregated Mono-6-(Alkylamino)-.Beta.-Cyclodextrins. J. Am. Chem. Soc. 1990; 112:3860–3868.
45. Protasenko V, Hull KL, Kuno M. Demonstration of a Low-Cost, Single-Molecule Capable, Multimode Optical Microscope. Chem. Educator. 2005; 10:269–282.

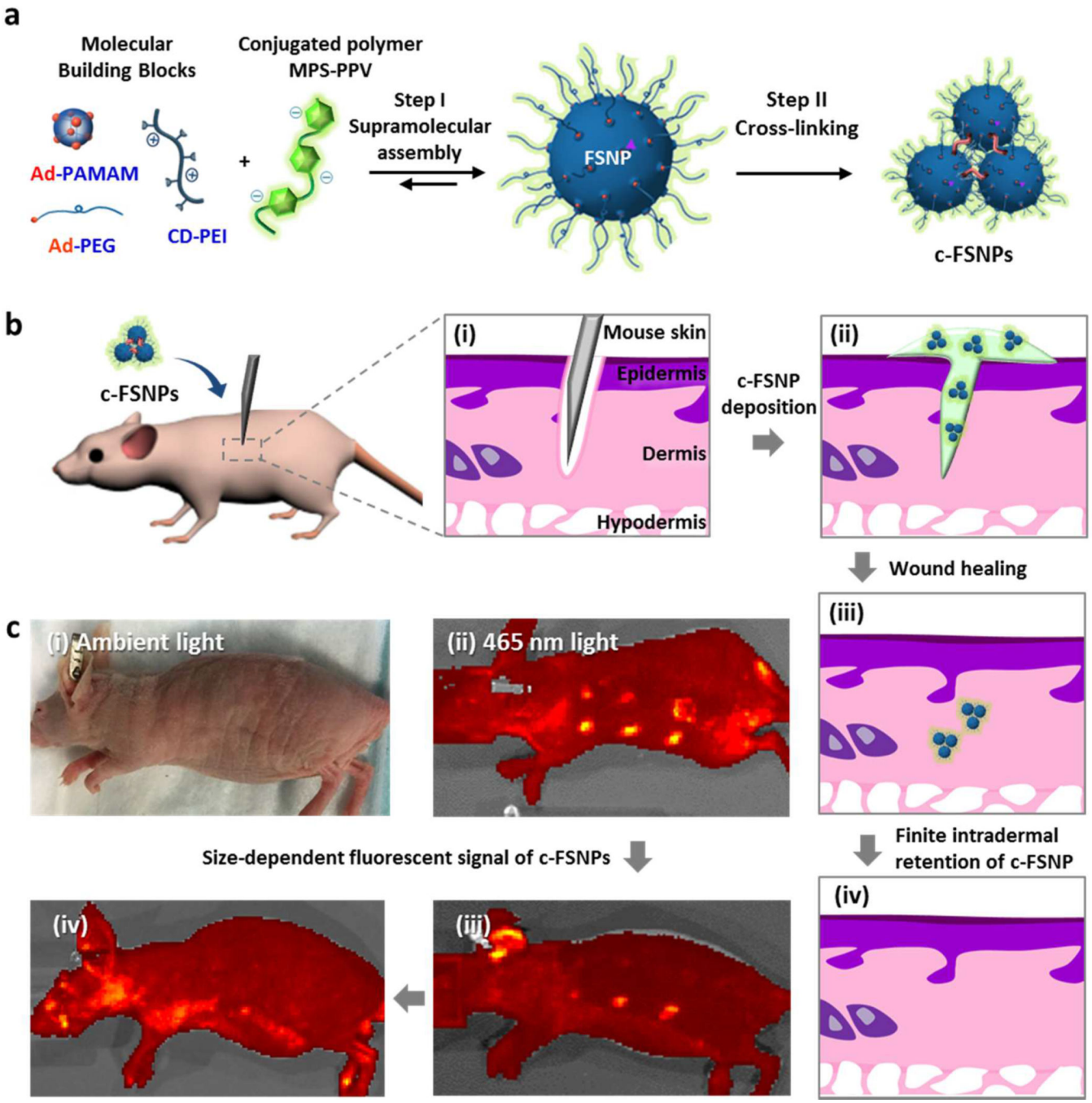

Figure 1.

c-FSNPs as “finite tattoo” pigments. (a) Two-step synthetic process employed for the preparation of c-FSNPs as “finite tattoo” pigments. (i) Step I: Supramolecular assembly of MPS-PPV and three molecular building blocks (*i.e.*, Ad-PAMAM, Ad-PEG, and CD-PEI) for the combinatorial formulation of different FSNPs. (ii) Step II: Cross-linking of FSNPs for the generation of micrometer-sized c-FSNPs. (b) Schematic illustration of the tattooing procedure by which c-FSNPs are deposited in the skin of a nu/nu mouse: (i) wound generation in the dermis layer of the mouse skin through poking with a needle, (ii)

deposition of c-FSNPs, (iii) wound healing, and (iv) clearance of tattooed c-FSNPs with a finite intradermal retention time. (c) Tattooed sites cannot be visualized (i) under ambient light irradiation, and their fluorescent signals can be detected (ii) under 465 nm light irradiation. (ii–iv) These tattooed c-FSNPs exhibited size-dependent fluorescent signals with finite intradermal retention times.

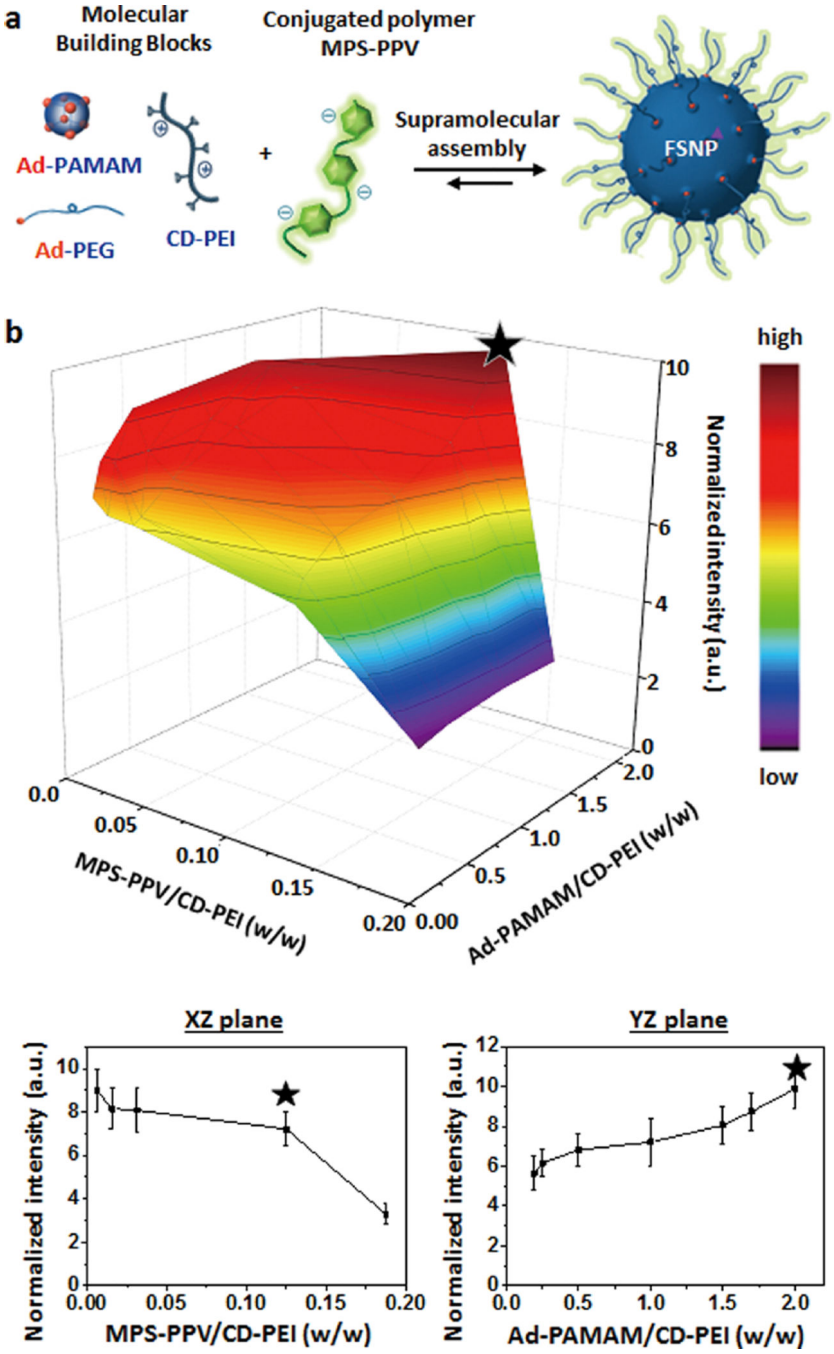

Figure 2.

(a) A small combinatorial library of FSNPs with 27 different formulations is achieved by performing supramolecular assembly of MPS-PPV and three molecular building blocks (*i.e.*, Ad-PAMAM, Ad-PEG, and CD-PEI) in different mixing ratios. (b) Three-dimensional profile of FSNPs' fluorescent intensities with variation (27 data points) of (i) MPS-PPV/CD-PEI ratio (w/w) and (ii) Ad-PAMAM/CD-PEI ratio (w/w). The fluorescent intensities of FSNPs are normalized to the observed intensities of free MPS-PPV of corresponding concentration for each FSNP formulation. The *XZ* and *YZ* planes across the optimal

performance present the normalized fluorescent intensity variation of FSNPs depending on MPS-PPV/CD-PEI ratio (w/w) and Ad-PAMAM/CD-PEI (w/w), respectively. The FSNPs exhibiting optimal fluorescent performance (⋆) are obtained with a specific formulation of the mixing ratio among the molecular building blocks, that is, MPS-PPV/CD-PEI ratio (w/w) = 0.125:1 and Ad-PAMAM/CD-PEI ratio (w/w) =2.0:1.

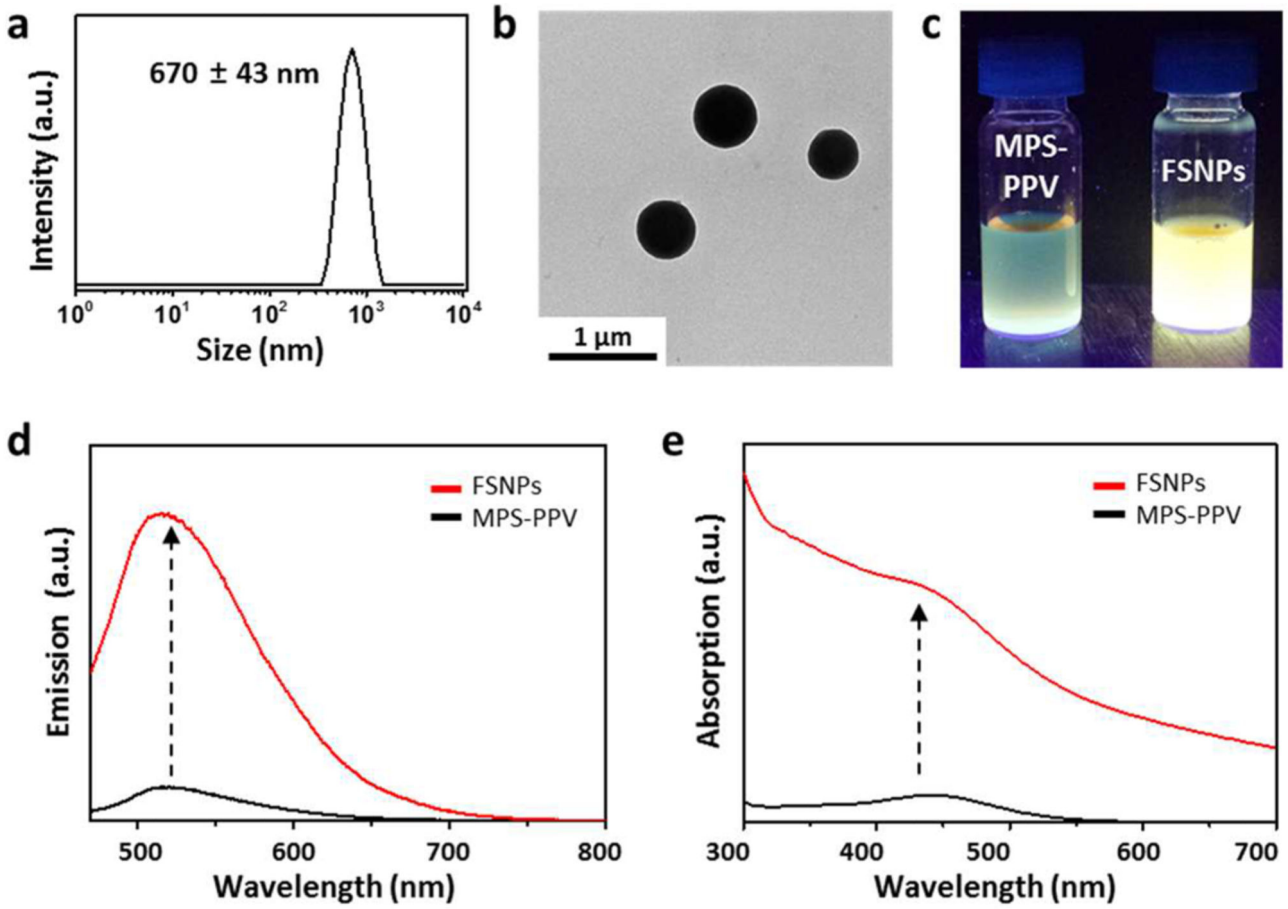

f

	Absorption/ Emission max	Absorption cross section (cm^{-2})*	Quantum yield (%)**	Fluorescent lifetime (ns)
MPS-PPV only	440/520 nm	1.72×10^{-17}	0.45	0.55, 2.11 ns
FSNPs	440/507 nm	1.17×10^{-16}	4.00	0.78, 2.08 ns

*All values were calculated based on the polymer unit of MPS-PPV.
** Relative quantum yield was calculated based on that of Cy3 standard.

Figure 3.

Characterization of FSNPs. (a) DLS data and (b) TEM image of the FSNPs selected from the combinatorial library (⋆, Figure 2b). The hydrodynamic size of the FSNPs, obtained by DLS, is 670 ± 43 nm, and TEM image reveals that FSNPs are homogeneous spherical nanoparticles. (c) Photograph of free MPS-PPV and the 670 nm sized FSNP solution with UV light irradiation (excitation = 365 nm). Comparison of (d) emission and (e) absorption spectrum of free MPS-PPV and the 670 nm sized FSNP. (f) Photophysical properties of free MPS-PPV and the 670 nm sized FSNP. All properties were calculated based on the repeating

unit of MPS-PPV. Dramatically enhanced fluorescence is observed with the 670 nm sized FSNPs which exhibits *ca.* 10-fold higher emission and *ca.* 6.8-fold higher absorption than free MPS-PPV.

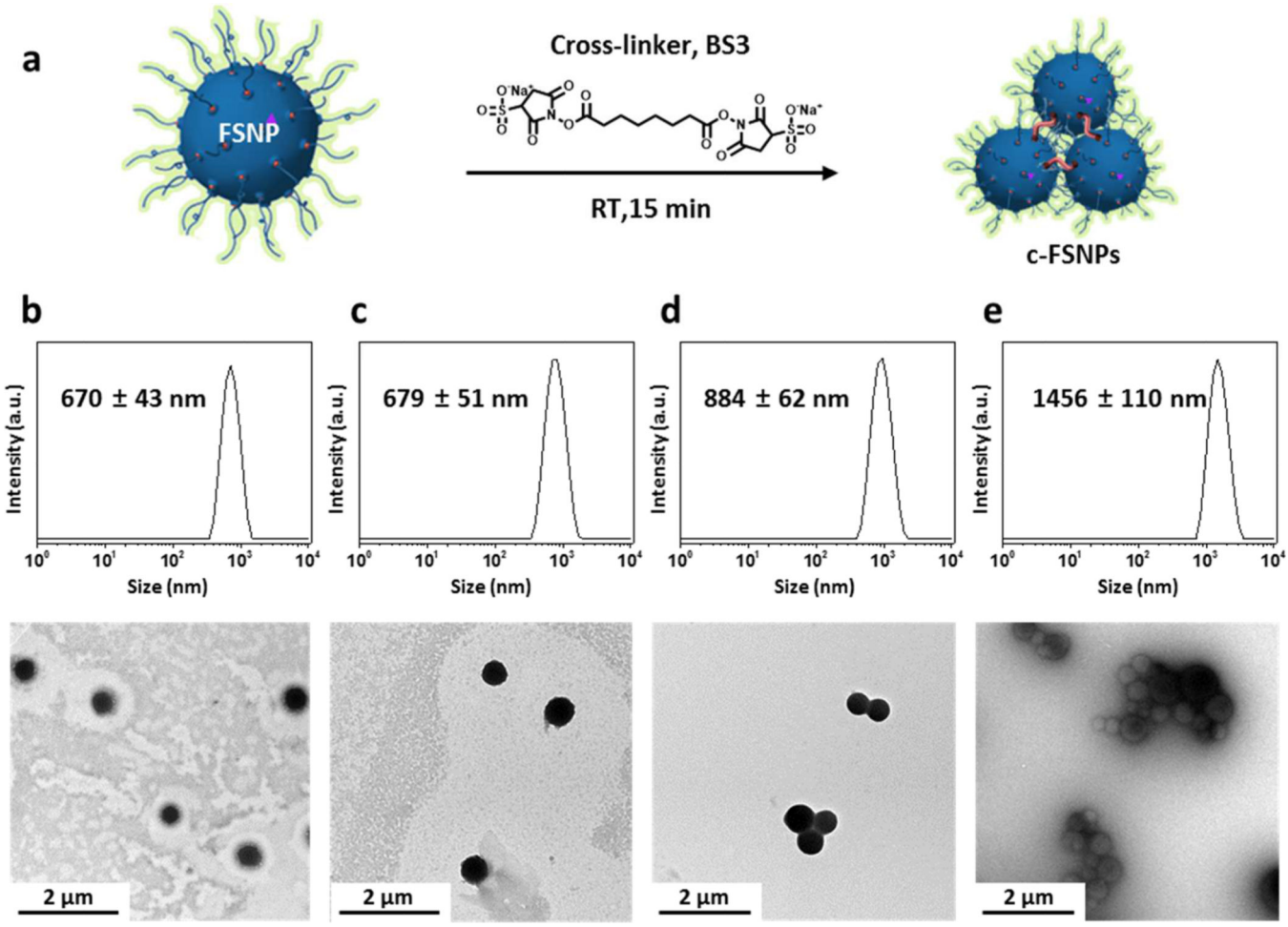

Figure 4.

Formation of cross-linked FSNPs. (a) Cross-linker, bis(sulfosuccinimidyl)suberate (BS3, 1–3 μg/mL) is introduced to the 670 nm sized FSNP solution to form micrometer-sized c-FSNPs. DLS data and TEM images of (b) 670 nm sized FSNPs and (c–e) c-FSNPs under the BS3 treatment with various concentrations: (c) 1 μg/mL, (2) 2 μg/mL, and (e) 3 μg/mL. Hydrodynamic size of the resulting c-FSNPs measured as 679 ± 51, 884 ± 62 and 1456 ± 110 nm when 1, 2, and 3 μg/mL of BS3 was introduced to the 670 nm sized FSNP solution, respectively. TEM images reveal that the resulting c-FSNPs are composed of clusters of 670 nm sized FSNPs maintaining their size and morphology.

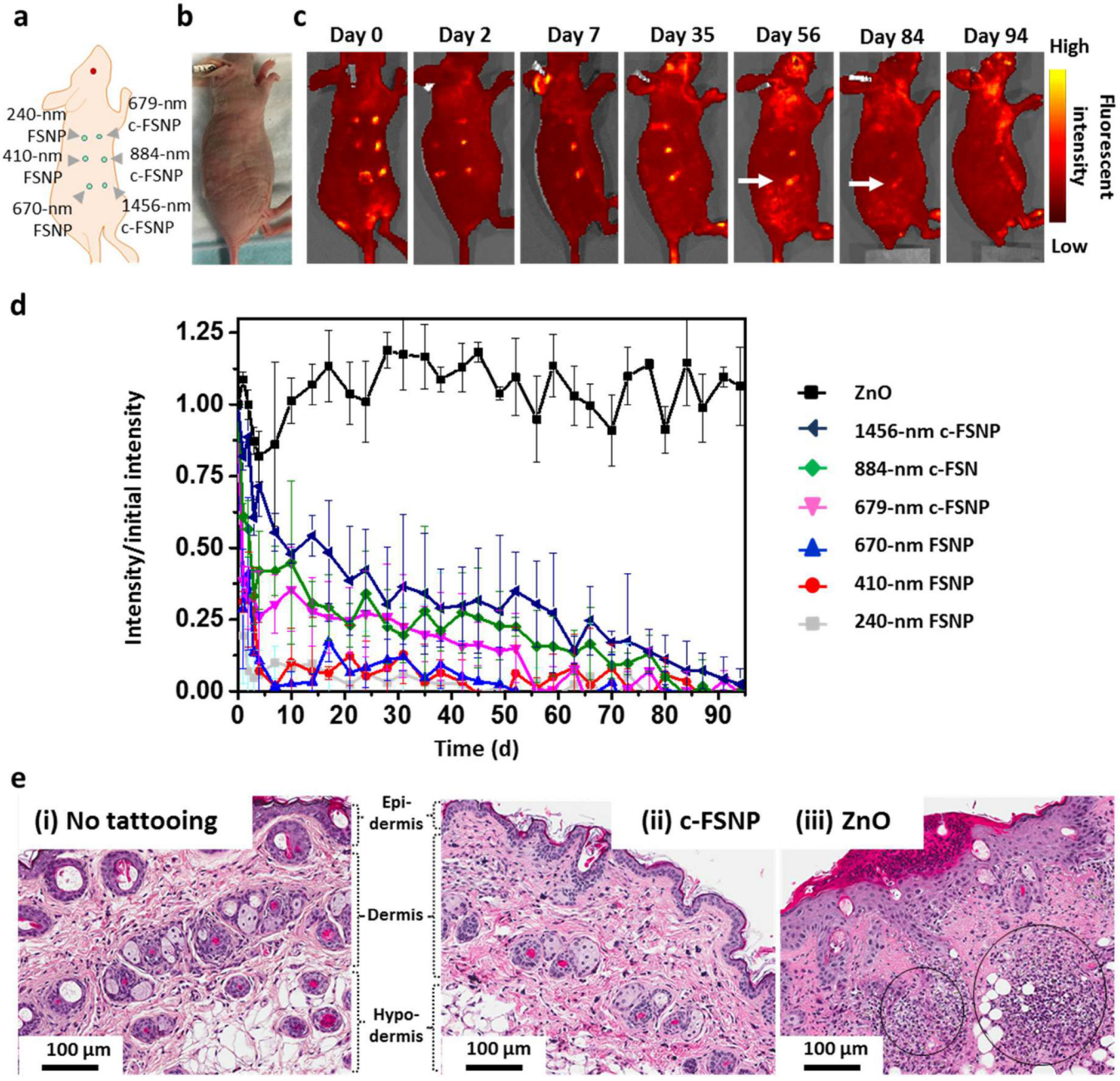

Figure 5.

Size-dependent intradermal retention study of FSNPs and c-FSNPs. (a) Three different-sized c-FSNPs (*i.e.*, 679, 884, and 1456 nm) along with three different-sized FSNPs (*i.e.*, 240, 410, and 670 nm), each containing 0.75 μg of MPS-PPV, are tattooed at six different locations on the back of the nu/nu mice ($n = 3$). (b) Photograph of a mouse tattooed with various-sized FSNPs and c-FSNPs under ambient light irradiation. (c) Fluorescent images of the tattooed mouse obtained using the *in vivo* optical imaging system (excitation/emission = 465/ 520 nm; exposure time = 2 s), for 94 days. (d) Time-dependent fluorescent signal of tattoo pigments, including a commercially available pigment (*i.e.*, ZnO), FSNPs, and c-FSNPs. The fluorescent signals are normalized to the initial fluorescent signal intensity at

day 0. In a long-term fluorescent signal observation up to 94 days, both FSNPs and c-FSNPs display a size-dependent fluorescent signal with a finite intradermal retention time. Among various FSNPs and c-FSNPs, 1456 nm sized c-FSNPs (arrow in panel c) show a fluorescent signal up to 84 days with the slowest fluorescent signal decay. The commercially available tattoo pigment, ZnO, exhibits a consistent fluorescent intensity over 94 days. (e) H&E stained skin sections from a nu/nu mouse tattooed with 1456 nm sized c-FSNPs after 2 days post-tattooing (100× magnification). Compared to (i) normal skin without tattooing, (ii) no obvious inflammation cells were observed in the skin of nu/nu mouse after c-FSNP tattooing. (iii) In contrast, commercially available tattoo pigments (*i.e.*, ZnO) attract a large population of inflammation cells (black circles).